Intermuscular adipose tissue (IMAT) directly modulates skeletal muscle insulin sensitivity in humans

Stephan Sachs[3], Simona Zarini[1], Darcy E. Kahn[1], Kathleen A. Harrison[1], Leigh Perreault[1], Tzu Phang[1], Sean A. Newsom[2], Allison Strauss[1], Anna Kerege[1], Jonathan A. Schoen[1], Daniel H. Bessesen[1], Thomas Schwarzmayr[4], Elisabeth Graf[4], Dominik Lutter[5,7], Jan Krumsiek[6], Susanna Hofmann[3,7,8], Bryan C. Bergman[1]

[1]University of Colorado Anschutz Medical Campus, Aurora, CO, USA
[2]Oregon State University, Corvallis, OR, USA
[3] Institute for Diabetes and Regeneration, Helmholtz Zentrum München, German Research Center for Environmental Health (GmbH), Neuherberg, Germany
[4]Institute of Human Genetics, Helmholtz Zentrum München, German Research Center for Environmental Health (GmbH), Neuherberg, Germany.
[5]Institute for Diabetes and Obesity, Helmholtz Diabetes Center at Helmholtz Zentrum München, German Research Center for Environmental Health (GmbH), 85764 Neuherberg, Germany
[6]Institute of Computational Biology, Helmholtz Zentrum München, Neuherberg 85764, Germany; German Center for Diabetes Research (DZD), Ingolstädter Landstr. 1, Neuherberg 85764, Germany.
[7]German Center for Diabetes Research (DZD), München-Neuherberg, Germany
[8]Medizinische Klinik and Poliklinik IV, Ludwig-Maximilians University, Munich, Germany

Running Head: IMAT in humans

Word Count
Abstract: 250
Main text: 3792
Tables: 2
Figures: 7
References: 51

Please address correspondence to:
Bryan C. Bergman, Ph.D.
Professor of Medicine
Division of Endocrinology, Metabolism, and Diabetes
University of Colorado Anschutz Medical Campus
PO Box 6511, MS 8106, Aurora, CO 80045
Bryan.Bergman@ucdenver.edu
303-724-3919

Abstract

Intermuscular adipose tissue (IMAT) is negatively related to insulin sensitivity, but a causal role of IMAT in the development of insulin resistance is unknown. IMAT was sampled in humans to test for the ability to induce insulin resistance *in vitro*, and characterize gene expression to uncover how IMAT may promote skeletal muscle insulin resistance. Human primary muscle cells were incubated with conditioned media from IMAT, visceral (VAT), or subcutaneous adipose tissue (SAT) to evaluate changes in insulin sensitivity. RNAseq analysis was performed on IMAT with gene expression compared to skeletal muscle and SAT, and relationships to insulin sensitivity determined in men and women spanning a wide range of insulin sensitivity measured by hyperinsulinemic-euglycemic clamp. Conditioned media from IMAT and VAT decreased insulin sensitivity similarly compared to SAT. Multidimensional scaling analysis revealed distinct gene expression patterns in IMAT compared to SAT and muscle. Pathway analysis revealed IMAT expression of genes in insulin signaling, oxidative phosphorylation, and peroxisomal metabolism related positively to donor insulin sensitivity, while expression of macrophage markers, inflammatory cytokines, and secreted extracellular matrix proteins were negatively related to insulin sensitivity. Perilipin 5 gene expression suggested greater IMAT lipolysis in insulin resistant individuals. Combined, these data show that factors secreted from IMAT modulate muscle insulin sensitivity, possibly via secretion of inflammatory cytokines and extracellular matrix proteins, and by increasing local FFA concentration in humans. These data suggest IMAT may be an important regulator of skeletal muscle insulin sensitivity, and could be a novel therapeutic target for skeletal muscle insulin resistance.

Keywords: Insulin sensitivity, myosteatosis, EMCL, adipose tissue distribution

Introduction

Intermuscular adipose tissue (IMAT) is marbled within skeletal muscle and accounts for less than 5% of total thigh fat, but directly relates to insulin resistance, subclinical atherosclerosis, and metabolic syndrome (18, 20, 49). The first report showing IMAT content was negatively related to insulin sensitivity was published in 2000 (20), and has been reinforced by nearly every investigation in this area across a wide range of muscle groups and individuals (6, 15, 18, 19, 35, 46, 48). IMAT content is negatively related to insulin sensitivity in many populations, including in men compared to women (6), African-Americans compared to Caucasians (15), and older compared to younger individuals (48). Unlike intramuscular triglyceride, IMAT is low in insulin sensitive endurance trained athletes (26), consistent with a negative relationship of IMAT to insulin sensitivity. Lifestyle interventions that increase insulin sensitivity either prevent IMAT accretion or reduce IMAT content while detraining increases IMAT content (11, 14, 21, 27, 37, 40). Combined, these data suggest IMAT may influence muscle insulin sensitivity. Although IMAT is uniquely positioned to influence muscle metabolism and insulin sensitivity by bathing muscle with hormones, adipokines, proteins, and free fatty acids, little is known about potential mechanisms by which IMAT may influence adjacent tissues due to the difficulty of accessing it.

Signaling and secretory properties of other adipose tissue depots such as subcutaneous and visceral fat play key roles in the induction of insulin resistance, inflammation, and tissue dysfunction (22, 30). To date, we know adipose tissue secretes nearly 300 proteins, which act as endocrine, paracrine, and autocrine signals

(30). Because of its physical proximity to skeletal muscle, IMAT may be a key factor regulating muscle insulin resistance and metabolic dysfunction, without measurable changes in systemic blood concentrations. Such proximity also means that therapeutic interventions directed at IMAT may powerfully alter muscle insulin sensitivity, and metabolic dysfunction. To date, IMAT has not been characterized in detail, so how interventions could be directed at IMAT are not known.

The purpose of this study was to directly sample IMAT in humans with a wide range of insulin sensitivities to directly test if IMAT induces insulin resistance *in vitro*, and to characterize IMAT gene expression to gain insight into how IMAT may promote skeletal muscle insulin resistance.

Methods

Subjects

Seven lean endurance trained athletes (athletes), 7 lean sedentary controls (lean), 21 sedentary obese individuals (obese), and 6 individuals with type 2 diabetes (T2D) were included in this study for IMAT conditioned media and RNAseq analysis. Skeletal muscle biopsies were also used for RNAseq analysis from 12 lean individuals in this study. In a separate cohort of 10 lean men and women that has been previously described (2), gluteal subcutaneous adipose tissue (SAT) was biopsied using needle aspiration after a 12-hour fast and used for RNAseq analysis (4). Conditioned media was generated from visceral (VAT) and SAT biopsies obtained from 7 obese individuals who were undergoing gastric bypass surgery. Subjects gave written informed consent,

and were excluded if they: had a body mass index (BMI) < 20 kg/m^2 or > 25 kg/m^2 for lean and athletes, and BMI <30 for obese and T2D, or had fasting triglycerides >150mg/dl, liver, kidney, thyroid, or lung disease. Sedentary subjects were engaged in planned physical activity < 2 hours/week. Endurance athletes were masters athletes training for cycling and triathlon competitions. Individuals with type 2 diabetes were excluded from the study if they used insulin and/or thiazolidinediones. All other medications were permissible, but washed out for two weeks prior to metabolic testing. Volunteers in other groups were not taking medications. Subjects were weight stable in the 6 months prior to the study. This study was approved by the Colorado Multiple Institution Review Board at the University of Colorado.

Preliminary Testing

Subjects reported to the Clinical Translational Research Center (CTRC) for screening procedures following a 12-hour overnight fast, where they were given a health and physical examination, followed by a fasting blood draw. Volunteers underwent a standard 75g oral glucose tolerance test to verify glucose tolerance. Percent body fat and leg lean mass was determined using DEXA analysis (Lunar DPX-IQ, Lunar Corporation, Madison, WI).

Exercise Control

Subjects were asked to refrain from planned physical activity for 48 hours before the metabolic study.

137

138 *Insulin Clamp Study*

139 Volunteers spent the night on the CTRC to ensure compliance with the overnight
140 fast. After a 12-hour overnight fast, an antecubital vein was cannulated in one arm for
141 infusions of insulin, [6,6-$^2H_2$]glucose, and dextrose, and a retrograde dorsal hand vein
142 was catheterized in the contralateral side for blood sampling via the heated hand
143 technique. A primed continuous infusion of [6,6-$^2H_2$]glucose was initiated at 0.04
144 mg/kg/min and continued throughout a 2-hour equilibrium period and the 3-hour
145 insulin clamp. After 2 hours of tracer equilibration, a percutaneous needle biopsy was
146 taken from midway between the greater trochanter of the femur and the patella. In a
147 subset of obese individuals, IMAT sampled from the vastus lateralis was immediately
148 washed in PBS and saved to generate conditioned media. In all other subjects, muscle
149 was immediately flash frozen in liquid nitrogen and stored at -80^{o}C until IMAT
150 dissection described below. A hyperinsulinemic-euglycemic clamp was then initiated
151 and continued for the next 3 hours using the method of DeFronzo et al (10) as previously
152 described for this cohort (39). Briefly, a primed continuous infusion of insulin was
153 administered at 40 mU/m^2/min for 3 hours. A variable infusion of 20% dextrose was
154 infused to maintain blood glucose ~90 mg/dl. The dextrose infusion used to maintain
155 euglycemia was labeled with [6,6-$^2H_2$]glucose (Cambridge Isotope Labs, Tewksbury,
156 MA) to maintain stable enrichment of plasma glucose. Glucose rate of disappearance
157 (glucose Rd) was calculated as previously described (12).

158

159 *Conditioned media experiments*

160 IMAT was sampled from the vastus lateralis while obtaining muscle biopsies in 7
161 obese individuals, immediately dissected away from skeletal muscle on ice using a
162 dissecting microscope, washed in PBS, and cultured in DMEM (1ml media/50mg
163 IMAT) for 48 hours at 37°C in 5% CO_2 to generate conditioned media. Conditioned
164 media was generated in the same way from VAT and SAT collected from individuals
165 undergoing gastric bypass surgery. For this comparison, patients with similar fasting
166 glucose, HbA1c, and age were chosen to minimize potential confounding variables.
167 IMAT, VAT, and SAT conditioned media was administered to primary myotubes from
168 a separate group of insulin resistant obese donors (n=5, Age: 36.2±2.1 yrs, BMI: 37.0±1.7
169 kg/m^2, sex:3M/2F, 3.8±0.9 mg/kg/min GIR during a 40mU/m^2/min insulin clamp)
170 during day 5-7 of differentiation at 5% of total media volume for 3.5 hours. Myotubes
171 were grown using standard techniques (16), while insulin sensitivity was determined
172 using an insulin stimulated glycogen synthesis assay using a final insulin concentration
173 of 100nM (45), and myotube lipid accumulation and conditioned media FFA content
174 measured as previously described (23). Data were normalized to the control condition
175 to account for differences in donor insulin sensitivity.

176

177 *Biopsy processing*

178 Flash frozen muscle biopsies were cut into smaller 20-30mg pieces and dissected
179 on ice for 1-1.5 minutes to separate IMAT from skeletal muscle using a dissection
180 microscope. IMAT and skeletal muscle samples were not contaminated by other tissues

as observed under a dissecting scope prior to RNA extraction described below. No attempt was made to separate adipocytes from stromal vascular cells in the isolated IMAT as our goal was to examine IMAT as a complete tissue.

RNAseq

Total RNA was prepared from IMAT, skeletal muscle, and subcutaneous adipose tissue biopsies using the RNeasy Lipid Tissue Kit (QIAGEN®) according to the manufacture' s instructions. The quality of the isolated RNA was determined with the Agilent 2100 Bioanalyzer (RNA 6000 Nano Kit, Agilent). All samples had a RNA integrity number (RIN) value greater than 7. Samples were handled in a blinded fashion during the library preparation and sequencing process.

For library preparation, 300μg of total RNA per sample was used. RNA molecules were poly(A) selected, fragmented, and reverse transcribed with the Elute, Prime, Fragment Mix (Illumina Inc., San Diego, CA). End repair, A-tailing, adaptor ligation, and library enrichment were performed as described in the Low Throughput protocol of the TruSeq RNA Sample Prep Guide (Illumina Inc., San Diego, CA) using the Bravo Automated Liquid Handling Platform (Agilent Technologies, Santa Clara, CA). RNA libraries were assessed for quality and quantity with the Agilent 2100 Bioanalyzer and the Quant-iT PicoGreen dsDNA Assay Kit (Thermo Fisher, Waltham, MA). RNA libraries were sequenced as 100 bp paired-end runs on an Illumina HiSeq2500 platform. Primary analysis for base calling and quality scorning was performed using the Real-Time Analysis software (Illumina Inc., San Diego, CA).

Sequences were aligned against the hg19 genome and UCSC knownGene annotation assembly (GTF file) with GEM mapper (version 1.7.1) using standard parameters (except mismatches=0.04 and min-decoded-strata=2). Read counts were calculated using HTSeq-count (version 0.6.0) with the same annotation files as for mapping.

Statistical Analysis

Differences between groups and tissues were analyzed using a 1-way ANOVA (SPSS, Chicago, IL). When significant differences were detected, individual means were compared using Students t-tests to determine differences between groups. For RNAseq analysis, we followed the recently published workflow described by Law et al. to analyze data including the 'edgeR' and 'limma' package in R. Specifically, for the analysis of RNAseq data comparing SAT, muscle, and IMAT, raw counts were filtered using edgeR (raw counts ≥25 in ≥8 samples). The raw counts of the remaining 15,550 genes were converted to counts per million (CPM) and $\log_2$-counts per million (log-CPM) values using edgeR (43). Values were normalized by the method of trimmed mean of M-values (TMM) (44). Limma was used to make multidimensional (MDS) plots (42).

To correlate gene expression and glucose Rd during the clamp for the IMAT RNAseq data, one sample was excluded as no glucose Rd was available. We used genes with more than 25 counts ≥70% of the IMAT samples. 13476 genes passed the criteria and were used for down-stream analyses. All genes significantly correlated to glucose Rd were evaluated within the GAGE package in R (34). We used the 'pathview' package

to visualize the correlation coefficients within the pathways in R (33). *A priori* hypotheses for genes representing macrophages, cytokines, extracellular matrix, and perilipins were corrected for multiple comparisons using the Benjamini-Hochberg method. An alpha level of 0.05 was used for statistical significance.

Results

Demographic information for obese donors used in conditioned media experiments for IMAT, VAT, and SAT from are shown in Table 1a. Individuals in the SAT/VAT group were significantly more obese than the IMAT group ($p<0.05$). Demographics for lean individuals used to compare gene expression patterns of IMAT, skeletal muscle, and SAT are shown in Table 1b. All of the female and male subjects in this comparison were lean with similar BMI and % body fat between groups. The age of individuals from which SAT biopsies were obtained was significantly lower than the other groups ($p<0.05$). Demographic information for individuals used to compare differences in IMAT gene expression across a range of insulin sensitivities are shown in Table 1c. There were a roughly equal number of men and women in this study (17/18), with a similar proportion of each sex in all groups. The mean age was not significantly different between groups, with BMI and body fat significantly lower in lean controls and athletes by design. Glucose Rd during the insulin clamp was significantly different between each group except for the comparison between lean individuals and endurance trained athletes which was of borderline significance ($p=0.06$).

IMAT conditioned media decreases myotube insulin sensitivity

Conditioned media from IMAT, VAT, and SAT of obese patients were administered separately to primary myotubes from obese donors to evaluate if IMAT influences insulin sensitivity in skeletal muscle through secreted factors. In the control condition 100nM of insulin for 1 hour resulted in a 104±15% increase in insulin stimulated glycogen storage. IMAT and VAT conditioned media significantly decreased insulin sensitivity compared to conditioned media from SAT ($p=0.002$) and DMEM control ($p=0.003$, Figure 1A). The decrease in insulin sensitivity was not significantly different between IMAT and VAT. Conditioned media from SAT did not change insulin sensitivity compared to DMEM control. Effects of conditioned media on insulin sensitivity *in vitro* are not due to a "non-self" immune response because there are no immune cells in this primary culture model. These data indicate that factors secreted from IMAT decrease insulin sensitivity *in vitro* with a potency similar to VAT.

IMAT conditioned media increases myotube 1,2-diacylglycerol concentration

To evaluate mechanisms explaining the induction of insulin resistance *in vitro*, we administered conditioned media to myotubes to evaluate if SAT, VAT, and IMAT conditioned media altered bioactive lipid accumulation. We found that VAT and IMAT conditioned media significantly increased myotube 1,2-diacylglycerol (DAG) content, but did not result in significant changes in ceramides, dihydroceramides, sphingomyelins, glucosylceramides, or lactosylceramides (Figures 1B-1G). These data

suggest that the VAT and IMAT secretome promote insulin resistance by inducing 1,2-DAG accumulation in skeletal muscle.

Basal lipolytic rates of SAT, VAT, and IMAT

Conditioned media from SAT, VAT, and IMAT were lipid extracted and analyzed for free fatty acids (FFA) using lipidomics, with FFA release rates normalized to dry tissue weight. We found similar rates of basal lipolysis in VAT and IMAT, which were both significantly greater than SAT (Figure 1H). Composition analysis revealed the majority of the increased rates of lipolysis in VAT and IMAT could be explained by release of 16:0 and 18:0, with significantly greater rates of 18:1 and 18:2 release also found in VAT compared to SAT (Figure 1I).

IMAT has a gene expression pattern distinct from skeletal muscle and subcutaneous fat

A multi-dimensional scaling (MDS) plot in Figure 2 shows differences in gene expression between IMAT, muscle, and SAT based on the 1500 most divergent genes. All three tissues showed clearly separated expression profiles with all samples from one depot clustering together, with further grouping within adipose tissues based on sex. These results indicate that IMAT has a unique transcriptome, which is different from that of muscle and subcutaneous fat.

IMAT gene expression correlates with insulin sensitivity

291 The schematic of the workflow is depicted in Figure 3. Within the IMAT
292 transcriptome, 988 genes correlated negatively and 1234 genes correlated positively
293 with glucose Rd. We used significantly correlated genes to find enriched pathways
294 using the KEGG database. 54 pathways were identified containing at least 10
295 significantly enriched correlated genes (Table 2). Among these pathways, there were 8
296 pathways directly linked to the immune system and 4 pathways related to the
297 extracellular matrix and local fibrosis.
298
299 Analysis of IMAT signaling pathways associated with insulin sensitivity:
300 Pathway analysis showed the insulin signaling pathway for IMAT was positively
301 related to insulin sensitivity, with relationship of individual genes to glucose Rd shown
302 in Figure 4A. The JAK/STAT and MAPK signaling pathways in IMAT were negatively
303 related to insulin sensitivity with the relationship of individual genes to glucose Rd
304 shown in Figures 4B-C. These data suggest that IMAT insulin signaling parallels whole
305 body insulin sensitivity, and could be negatively influenced by inflammation through
306 the JAK/STAT and MAPK pathways. Insulin normally inhibits lipolysis in adipose
307 tissue, so insulin resistant IMAT could increase local release of free fatty acids into
308 interstitial fluid surrounding muscle. Pathway analysis revealed a positive relationship
309 of IMAT oxidative phosphorylation to insulin sensitivity (Figure 4D). These data
310 suggest insulin resistant IMAT may have decreased mitochondrial function and lipid
311 oxidation, which could also contribute to enhanced release of free fatty acids into
312 interstitial fluid surrounding muscle.

313

314 Macrophage marker and inflammatory cytokine gene expression:

315 Common macrophage marker genes were evaluated in IMAT, and we found
316 colony stimulating factor 1 (*CSF1),* cluster of differentiation 163 (*CD163),* monocyte
317 chemotactic protein 1 (*MCP1),* integrin subunit alpha M *(ITGAM),* colony stimulating
318 Factor 1 Receptor *(CSF1R),* integrin subunit alpha X (*ITGAX),* and C-type lectin domain
319 family 7 member A *(CLEC7A)* were negatively correlated to insulin sensitivity (Figure
320 5A). We found significant negative relationships between insulin sensitivity and several
321 inflammatory cytokines such as plasminogen activator inhibitor type 1 (*PAI-1)* and
322 *MCP1* (Figure 5B), while there were no significant relationships between IMAT anti-
323 inflammatory gene expression and insulin sensitivity. TNF alpha induced protein 3
324 (*TNFAIP3)* codes for a protein that limits TNFα induced NFκB inflammation(9), and
325 was also significantly related to glucose Rd. These data not only indicate that IMAT
326 contains macrophages proportional to insulin sensitivity, but also suggests that
327 macrophage cytokine secretion within IMAT is negatively related to insulin sensitivity.

328

329 Extracellular matrix gene expression:

330 Among the IMAT genes that strongly correlated with glucose Rd, the expression
331 of extracellular matrix genes collagen type XXIV alpha 1 (*COL24A1),* discoidin domain
332 receptor family, member 1 (*DDR1),* and connective tissue growth factor *(CTGF)* scaled
333 to insulin sensitivity (Figure 5C). There are many cell types in adipose tissue, including
334 fibroblasts, that may also contribute to extracellular matrix protein secretion (13).

335 Therefore, we evaluated the relationship of fibroblast markers fibroblast specific protein
336 1 (*FSP1),* prolyl 4-hydroxylase subunit alpha 2 *(P4HA2),* fibroblast activation protein
337 alpha *(FAP),* prolyl 4-hydroxylase subunit alpha 1 *(P4HA1)*, and prolyl 4-hydroxylase
338 subunit beta (*P4HB)* to insulin sensitivity and only found *FSP1* was significantly related
339 to insulin sensitivity after correcting for multiple comparisons (Figure 5C).
340
341 Lipolytic and peroxisome gene expression:
342 Expression of genes involved in regulating lipolysis were analyzed to evaluate
343 potential regulation of lipid droplet lipolysis in IMAT. Other than a significant
344 relationship between *PLIN5* and glucose Rd, there were no other significant
345 relationships to insulin sensitivity for genes regulating lipolysis (Figure 6A).
346 Additionally, there was a positive relationship of the KEGG 'Peroxisome' pathway to
347 insulin sensitivity (Figure 6B). We did not find significant differences between groups in
348 gene expression for pathways of beta-oxidation or triglyceride re-esterification. While
349 we cannot exclude alterations in protein content or activity to these pathways, these
350 data suggest reduced peroxisome pathway expression may contribute to greater IMAT
351 FFA release in insulin resistant individuals.
352 A summary figure showing potential mechanisms by which IMAT may promote
353 decreased skeletal muscle insulin sensitivity implicated in this study are shown in
354 Figure 7.
355
356 Discussion

Due to its physical proximity, secreted FFA, proteins, and cytokines from IMAT are likely particularly potent for regulating muscle insulin sensitivity and metabolic function. Such proximity also means that therapeutic interventions directed at IMAT may powerfully alter muscle insulin sensitivity and metabolic dysfunction. However, specific components of IMAT signaling in humans that modify muscle metabolism are not known and, therefore, cannot be targeted by a therapeutic intervention. To our knowledge, this is the first publication to directly sample IMAT in humans in order to reveal how IMAT may impact muscle metabolism and insulin resistance. Key findings from this study include: conditioned media from IMAT decreased insulin sensitivity in primary human myotubes with a potency similar to VAT, administration of conditioned media from IMAT and VAT increased myotube 1,2-DAG content, VAT and IMAT have greater rates of basal lipolysis compared to SAT, expression of macrophage markers, inflammatory cytokines, and connective tissue markers in IMAT were significantly greater in insulin resistant individuals, and finally IMAT RNA expression in insulin resistant individuals was consistent with increased rates of IMAT lipolysis and interstitial FFA concentration leading to muscle lipid accumulation. These data provide the first direct evidence that factors secreted from IMAT contribute to the development of insulin resistance.

To date, studies in humans have been limited to associations between IMAT accumulation and metabolic outcomes due to the difficulty in sampling this tissue depot. To determine if skeletal muscle or SAT were collected in our IMAT samples, we compared gene expression patterns in skeletal muscle, IMAT, and SAT from lean

individuals. Our analyses revealed distinct gene expression patterns between these tissue depots, suggesting contamination between tissues was unlikely. Similar to what has been previously reported in livestock (8, 29), we interpret these data to suggest that IMAT is a separate tissue depot with a unique gene expression signature that differs markedly from skeletal muscle and subcutaneous adipose tissue in humans.

Our functional *in vitro* experiments show IMAT and VAT secreted factors that decreased muscle insulin sensitivity relative to SAT. The components of IMAT conditioned media causing insulin resistance are not known. However, the transcriptomic signature of IMAT suggests it may contain macrophages that secrete inflammatory cytokines and could promote local inflammation in skeletal muscle. These data also support the idea that IMAT may secrete proteins that influence the extracellular matrix, and could increase local FFA concentration, both of which are known to impact muscle insulin sensitivity (50). Our data show that IMAT and VAT conditioned media increased muscle cell accumulation of 1,2-DAG, which is known to decrease insulin signaling and sensitivity through activation of novel PKC isoforms, and may help explain the insulin resistance observed *in vitro*. These ideas are supported by a recent study showing conditioned media from fibro-adipogenic precursors differentiated into adipocytes decreased insulin sensitivity and signaling in primary muscle cell cultures (28). Together, these data indicate that secretions from IMAT can decrease muscle insulin sensitivity similar to VAT, and suggest that the IMAT secretome bathes the muscle in factors that attenuate insulin sensitivity.

While exact mechanisms by which IMAT promotes insulin resistance are unknown, the initial report by Goodpaster et al. suggested IMAT may induce insulin resistance by impairing muscle blood flow, insulin diffusion capacity, or increasing local FFA concentration (20). Our data support the concept that IMAT triglyceride lipolysis may increase interstitial FFA concentration leading to insulin resistance. This idea is supported by human microdialysis studies showing that obese compared to lean individuals have greater interstitial glycerol concentrations (5, 47), and that individuals with Type 2 Diabetes compared with normal glucose tolerant controls have less inhibition of muscle and IMAT lipolysis in response to insulin (24). Additionally, when compared to SAT, lipolysis in muscle and IMAT is less inhibited in response to insulin (7, 36, 47) and increases more in response to fasting (17). IMAT mRNA expression of genes controlling lipolysis did not reveal coordinated changes suggestive of increased capacity for IMAT lipolysis in insulin resistant individuals. However, basal lipolytic rates were significantly greater in VAT and IMAT compared to SAT. These data suggest that regulation of lipolysis, rather than capacity for lipolysis, may explain differences in basal lipolytic rates measured between tissues *in vitro*. IMAT's high lipolytic activity and close proximity to muscle mean that it likely plays an important role in regulating local FFA concentration, and the increase in muscle interstitial glycerol found in insulin resistant individuals.

Similar to a report on fibro-adipogenic precursors from human skeletal muscle (1), our data suggest IMAT insulin sensitivity parallels whole body insulin sensitivity. Similar to reports of adipose tissue insulin resistance in other studies (3, 24), decreased

IMAT insulin sensitivity would attenuate insulin-inhibition of lipolysis and also contribute to increased interstitial FFA concentration. Moreover, we found key genes of the peroxisomal beta-oxidation pathway to be down-regulated in obesity and T2D. If there were no adaptive increases in mitochondrial beta-oxidation or re-esterification, this could contribute to increased interstitial FFA concentration (32). Together, these findings suggest IMAT may explain increased muscle lipolytic rates found in obese individuals that promote increased interstitial FFA concentration, leading to muscle lipid accumulation, and ultimately decreased muscle insulin sensitivity.

Visceral adipose tissue is thought to be uniquely deleterious towards insulin sensitivity (41). Importantly, the relationship between IMAT and insulin resistance is almost equally as strong as for VAT (51), and our conditioned media data revealed that the secretome of IMAT and VAT have a similar ability to decrease insulin sensitivity. Animal studies found low expression of mRNA for oxidative metabolism, and high expression of inflammatory cytokines in IMAT (29), as well as similar DNA methylation in VAT and IMAT with increased expression of *IL-6*, *TNFα*, and *PAI-1* compared to subcutaneous adipose tissue (31). Therefore, it appears that IMAT is a uniquely regulated tissue which is functionally similar to VAT, and is capable of secreting cytokines known to influence tissue inflammation and function. We found that *PAI-1* and *MCP1* gene expression scaled to insulin resistance, as did *TNFAIP3*, which codes for a protein that limits TNFα induced NFκB inflammation (9). Therefore, IMAT may be both a target and a source of inflammation in insulin resistant humans.

443 The ability of IMAT to expand is limited by the morphology of muscle, and we
444 reasoned may also be limited by the extracellular matrix (ECM), which is known to
445 influence insulin sensitivity in adipose tissue, liver, and skeletal muscle (25, 50). It is
446 possible that IMAT, being contained with the muscle fascia, may also be an example of
447 adipose tissue with limitations for expansion with negative effects on insulin sensitivity.
448 Our data indicate IMAT may secrete proteins that modify muscle ECM and decrease
449 insulin sensitivity in humans. Therefore, IMAT may increase muscle fibrosis, and could
450 influence the development of sarcopenia, age-related metabolic dysfunction, as well as
451 the greater declines in these parameters in individuals with type 2 diabetes (38).
452 There are several limitations to this work. Individuals in our SAT group were
453 significantly younger compared to the IMAT and skeletal muscle cohort making it
454 possible that the differences shown in Figure 2 could be influenced by age. We do not
455 have any measurements of total IMAT content in these volunteers, and therefore cannot
456 determine if IMAT gene expression was related to IMAT content to understand the
457 biology of this tissue. Flash frozen skeletal muscle biopsies from which IMAT was
458 isolated for RNAseq analysis were thawed and quickly dissected on ice, which may
459 have influenced the gene expression profile. We did not separate IMAT into various cell
460 types as we wanted to study the tissue as a whole. It would have been ideal to measure
461 stimulated IMAT lipolysis to evaluate the potential impact on muscle lipid delivery.
462 Unfortunately, fresh tissue was not available for these measurements. Every attempt
463 was made to prevent muscle contamination of IMAT, but it is possible that muscle was
464 also measured along with IMAT in these analyses.

These data represent the first direct sampling and analysis of IMAT in humans. IMAT conditioned media decreased insulin sensitivity and caused accumulation of 1,2-DAG in primary myotubes with a potency similar to VAT. These data indicate that factors secreted by IMAT can contribute to the development of muscle insulin resistance. We found IMAT mRNA expression consistent with macrophage infiltration, cytokine and extracellular matrix secretion, and decreased insulin signaling. Collectively, these data indicate that IMAT may be an important regulator of skeletal muscle insulin sensitivity whose importance we are just starting to appreciate.

Acknowledgements

Some of these data were presented as an abstract at the ADA 77th Scientific Sessions in San Diego, CA, USA, June 9-13, 2017.

Funding

This work was partially supported by the National Institutes of Health General Clinical Research Center grant RR-00036, National Institute of Diabetes and Digestive and Kidney Diseases (NIDDK) grant to Bryan C. Bergman (R01DK089170), T32 DK07658 grant to Nancy Krebs, the Colorado Nutrition Obesity Research Center grant P30DK048520, the Helmholtz Alliance ICEMED (Imaging and Curing Environmental Metabolic Diseases), the Network Fund of the Helmholtz Association and the German Center for Diabetes Research (DZD).

Dualities of interest

Nothing to report.

Contribution Statement

S.S. performed the RNA extraction and RNAseq analyses, and help write and edit the manuscript, S.Z. generated conditioned media, performed the insulin sensitivity in vitro experiments, and edited and help write the manuscript, D.K. performed experiments administering conditioned media to muscle cells in vitro as well as measured conditioned media FFA content, and edited and help write the manuscript, K.A.H. performed all lipidomic extractions and analyses and edited and help write the manuscript, L.P. helped design the study, provided medical oversight, performed all biopsies, and helped write the manuscript, J.S.B performed the PCA and statistical analyses for this manuscript, and edited and help write the manuscript, T.S., D.L, and T.P. performed RNAseq data analyses and statistics, and edited and help write the manuscript, J.K. performed RNAseq data statistics, edited and help write the manuscript, E.G. performed RNAseq, S.N. helped with subject testing, and edited and help write the manuscript, A.S. helped with subject testing, and edited the manuscript, A.K. performed subject testing, analyzed samples, and edited the manuscript, J.S. harvested the subcutaneous adipose tissue during surgery and edited the manuscript, D.B. performed the subcutaneous adipose tissue biopsies and edited the manuscript, S.H. helped perform the RNAseq analyses, edited and help write the manuscript, B.C.B.

designed the study, performed subject testing, analyzed data, and wrote the manuscript. B.C.B is the guarantor of this work and, as such, had full access to all the data in the study and takes responsibility for the integrity of the data and the accuracy of the data analysis.

References

1. **Arrighi N, Moratal C, Clement N, Giorgetti-Peraldi S, Peraldi P, Loubat A, Kurzenne JY, Dani C, Chopard A, and Dechesne CA**. Characterization of adipocytes derived from fibro/adipogenic progenitors resident in human skeletal muscle. *Cell Death Dis* 6: e1733, 2015.
2. **Bergman BC, Cornier MA, Horton TJ, and Bessesen D**. Effects Of Fasting On Insulin Action And Glucose Kinetics In Lean And Obese Men And Women. *Am J Physiol* 293: E1103-1111, 2007.
3. **Bergman BC, Howard D, Schauer IE, Maahs DM, Snell-Bergeon JK, Clement TW, Eckel RH, Perreault L, and Rewers M**. The importance of palmitoleic acid to adipocyte insulin resistance and whole-body insulin sensitivity in type 1 diabetes. *The Journal of clinical endocrinology and metabolism* 98: E40-50, 2013.
4. **Bessesen DH, Cox-York KA, Hernandez TL, Erickson CB, Wang H, Jackman MR, and Van Pelt RE**. Postprandial triglycerides and adipose tissue storage of dietary fatty acids: impact of menopause and estradiol. *Obesity (Silver Spring)* 23: 145-153, 2015.
5. **Blaak EE, Schiffelers SL, Saris WH, Mensink M, and Kooi ME**. Impaired beta-adrenergically mediated lipolysis in skeletal muscle of obese subjects. *Diabetologia* 47: 1462-1468, 2004.
6. **Boettcher M, Machann J, Stefan N, Thamer C, Haring HU, Claussen CD, Fritsche A, and Schick F**. Intermuscular adipose tissue (IMAT): association with other adipose tissue compartments and insulin sensitivity. *Journal of magnetic resonance imaging : JMRI* 29: 1340-1345, 2009.
7. **Bolinder J, Kerckhoffs DA, Moberg E, Hagstrom-Toft E, and Arner P**. Rates of skeletal muscle and adipose tissue glycerol release in nonobese and obese subjects. *Diabetes* 49: 797-802, 2000.
8. **Bong JJ, Cho KK, and Baik M**. Comparison of gene expression profiling between bovine subcutaneous and intramuscular adipose tissues by serial analysis of gene expression. *Cell biology international* 34: 125-133, 2010.
9. **Coornaert B, Carpentier I, and Beyaert R**. A20: central gatekeeper in inflammation and immunity. *J Biol Chem* 284: 8217-8221, 2009.
10. **DeFronzo RA, Tobin JD, and Andres R**. Glucose clamp technique: a method for quantifying insulin secretion and resistance. *Am J Physiol* 237: E214-223, 1979.
11. **Durheim MT, Slentz CA, Bateman LA, Mabe SK, and Kraus WE**. Relationships between exercise-induced reductions in thigh intermuscular adipose tissue, changes in lipoprotein particle size, and visceral adiposity. *Am J Physiol Endocrinol Metab* 295: E407-412, 2008.
12. **Finegood DT, Bergman RN, and Vranic M**. Estimation of endogenous glucose production during hyperinsulinemic-euglycemic glucose clamps. Comparison of unlabeled and labeled exogenous glucose infusates. *Diabetes* 36: 914-924, 1987.
13. **Frantz C, Stewart KM, and Weaver VM**. The extracellular matrix at a glance. *J Cell Sci* 123: 4195-4200, 2010.

14. **Gallagher D, Heshka S, Kelley DE, Thornton J, Boxt L, Pi-Sunyer FX, Patricio J, Mancino J, Clark JM, and Group MRIASGoLAR**. Changes in adipose tissue depots and metabolic markers following a 1-year diet and exercise intervention in overweight and obese patients with type 2 diabetes. *Diabetes Care* 37: 3325-3332, 2014.
15. **Gallagher D, Kuznia P, Heshka S, Albu J, Heymsfield SB, Goodpaster B, Visser M, and Harris TB**. Adipose tissue in muscle: a novel depot similar in size to visceral adipose tissue. *Am J Clin Nutr* 81: 903-910, 2005.
16. **Gaster M, Kristensen SR, Beck-Nielsen H, and Schroder HD**. A cellular model system of differentiated human myotubes. *APMIS* 109: 735-744, 2001.
17. **Gjedsted J, Gormsen LC, Nielsen S, Schmitz O, Djurhuus CB, Keiding S, Orskov H, Tonnesen E, and Moller N**. Effects of a 3-day fast on regional lipid and glucose metabolism in human skeletal muscle and adipose tissue. *Acta physiologica* 191: 205-216, 2007.
18. **Goodpaster BH, Krishnaswami S, Harris TB, Katsiaras A, Kritchevsky SB, Simonsick EM, Nevitt M, Holvoet P, and Newman AB**. Obesity, regional body fat distribution, and the metabolic syndrome in older men and women. *Arch Intern Med* 165: 777-783, 2005.
19. **Goodpaster BH, Krishnaswami S, Resnick H, Kelley DE, Haggerty C, Harris TB, Schwartz AV, Kritchevsky S, and Newman AB**. Association between regional adipose tissue distribution and both type 2 diabetes and impaired glucose tolerance in elderly men and women. *Diabetes Care* 26: 372-379, 2003.
20. **Goodpaster BH, Thaete FL, and Kelley DE**. Thigh adipose tissue distribution is associated with insulin resistance in obesity and in type 2 diabetes mellitus. *Am J Clin Nutr* 71: 885-892, 2000.
21. **Greco AV, Mingrone G, Giancaterini A, Manco M, Morroni M, Cinti S, Granzotto M, Vettor R, Camastra S, and Ferrannini E**. Insulin resistance in morbid obesity: reversal with intramyocellular fat depletion. *Diabetes* 51: 144-151, 2002.
22. **Hardin BJ, Campbell KS, Smith JD, Arbogast S, Smith J, Moylan JS, and Reid MB**. TNF-alpha acts via TNFR1 and muscle-derived oxidants to depress myofibrillar force in murine skeletal muscle. *J Appl Physiol (1985)* 104: 694-699, 2008.
23. **Harrison KA, and Bergman BC**. HPLC-MS/MS Methods for Diacylglycerol and Sphingolipid Molecular Species in Skeletal Muscle. In: *High Throughput Metabolomics and Protocols*, edited by D'Alessandro ASpringer Nature, 2019.
24. **Jocken JW, Goossens GH, Boon H, Mason RR, Essers Y, Havekes B, Watt MJ, van Loon LJ, and Blaak EE**. Insulin-mediated suppression of lipolysis in adipose tissue and skeletal muscle of obese type 2 diabetic men and men with normal glucose tolerance. *Diabetologia* 56: 2255-2265, 2013.
25. **Khan T, Muise ES, Iyengar P, Wang ZV, Chandalia M, Abate N, Zhang BB, Bonaldo P, Chua S, and Scherer PE**. Metabolic dysregulation and adipose tissue fibrosis: role of collagen VI. *Mol Cell Biol* 29: 1575-1591, 2009.
26. **Kim J, Heshka S, Gallagher D, Kotler DP, Mayer L, Albu J, Shen W, Freda PU, and Heymsfield SB**. Intermuscular adipose tissue-free skeletal muscle mass: estimation by dual-energy X-ray absorptiometry in adults. *J Appl Physiol (1985)* 97: 655-660, 2004.

27. **Konopka AR, Wolff CA, Suer MK, and Harber MP**. Relationship between Intermuscular Adipose Tissue Infiltration and Myostatin before and after Aerobic Exercise Training. *Am J Physiol Regul Integr Comp Physiol* 2018.
28. **Laurens C, Louche K, Sengenes C, Coue M, Langin D, Moro C, and Bourlier V**. Adipogenic progenitors from obese human skeletal muscle give rise to functional white adipocytes that contribute to insulin resistance. *Int J Obes (Lond)* 40: 497-506, 2016.
29. **Lee HJ, Park HS, Kim W, Yoon D, and Seo S**. Comparison of Metabolic Network between Muscle and Intramuscular Adipose Tissues in Hanwoo Beef Cattle Using a Systems Biology Approach. *International journal of genomics* 2014: 679437, 2014.
30. **Lehr S, Hartwig S, Lamers D, Famulla S, Muller S, Hanisch FG, Cuvelier C, Ruige J, Eckardt K, Ouwens DM, Sell H, and Eckel J**. Identification and validation of novel adipokines released from primary human adipocytes. *Molecular & cellular proteomics : MCP* 11: M111 010504, 2012.
31. **Li M, Wu H, Wang T, Xia Y, Jin L, Jiang A, Zhu L, Chen L, Li R, and Li X**. Co-methylated genes in different adipose depots of pig are associated with metabolic, inflammatory and immune processes. *International journal of biological sciences* 8: 831-837, 2012.
32. **Lodhi IJ, and Semenkovich CF**. Peroxisomes: a nexus for lipid metabolism and cellular signaling. *Cell Metab* 19: 380-392, 2014.
33. **Luo W, and Brouwer C**. Pathview: an R/Bioconductor package for pathway-based data integration and visualization. *Bioinformatics* 29: 1830-1831, 2013.
34. **Luo W, Friedman MS, Shedden K, Hankenson KD, and Woolf PJ**. GAGE: generally applicable gene set enrichment for pathway analysis. *BMC Bioinformatics* 10: 161, 2009.
35. **Miljkovic-Gacic I, Gordon CL, Goodpaster BH, Bunker CH, Patrick AL, Kuller LH, Wheeler VW, Evans RW, and Zmuda JM**. Adipose tissue infiltration in skeletal muscle: age patterns and association with diabetes among men of African ancestry. *Am J Clin Nutr* 87: 1590-1595, 2008.
36. **Moberg E, Sjoberg S, Hagstrom-Toft E, and Bolinder J**. No apparent suppression by insulin of in vivo skeletal muscle lipolysis in nonobese women. *Am J Physiol Endocrinol Metab* 283: E295-301, 2002.
37. **Murphy JC, McDaniel JL, Mora K, Villareal DT, Fontana L, and Weiss EP**. Preferential reductions in intermuscular and visceral adipose tissue with exercise-induced weight loss compared with calorie restriction. *J Appl Physiol (1985)* 112: 79-85, 2012.
38. **Park SW, Goodpaster BH, Strotmeyer ES, de Rekeneire N, Harris TB, Schwartz AV, Tylavsky FA, and Newman AB**. Decreased muscle strength and quality in older adults with type 2 diabetes: the health, aging, and body composition study. *Diabetes* 55: 1813-1818, 2006.
39. **Perreault L, Newsom SA, Strauss A, Kerege A, Kahn DE, Harrison KA, Snell-Bergeon JK, Nemkov T, D'Alessandro A, Jackman MR, MacLean PS, and Bergman BC**. Intracellular localization of diacylglycerols and sphingolipids influences insulin sensitivity and mitochondrial function in human skeletal muscle. *JCI Insight* 3: 2018.

40. **Popadic Gacesa JZ, Kozic DB, and Grujic NG**. Triceps brachii strength and regional body composition changes after detraining quantified by MRI. *Journal of magnetic resonance imaging : JMRI* 33: 1114-1120, 2011.
41. **Pouliot MC, Despres JP, Nadeau A, Moorjani S, Prud'Homme D, Lupien PJ, Tremblay A, and Bouchard C**. Visceral obesity in men. Associations with glucose tolerance, plasma insulin, and lipoprotein levels. *Diabetes* 41: 826-834, 1992.
42. **Ritchie ME, Phipson B, Wu D, Hu Y, Law CW, Shi W, and Smyth GK**. limma powers differential expression analyses for RNA-sequencing and microarray studies. *Nucleic Acids Res* 43: e47, 2015.
43. **Robinson MD, McCarthy DJ, and Smyth GK**. edgeR: a Bioconductor package for differential expression analysis of digital gene expression data. *Bioinformatics* 26: 139-140, 2010.
44. **Robinson MD, and Oshlack A**. A scaling normalization method for differential expression analysis of RNA-seq data. *Genome Biol* 11: R25, 2010.
45. **Schmitz-Peiffer C, Craig DL, and Biden TJ**. Ceramide generation is sufficient to account for the inhibition of the insulin-stimulated PKB pathway in C2C12 skeletal muscle cells pretreated with palmitate. *J Biol Chem* 274: 24202-24210, 1999.
46. **Sinha R, Dufour S, Petersen KF, LeBon V, Enoksson S, Ma YZ, Savoye M, Rothman DL, Shulman GI, and Caprio S**. Assessment of skeletal muscle triglyceride content by (1)H nuclear magnetic resonance spectroscopy in lean and obese adolescents: relationships to insulin sensitivity, total body fat, and central adiposity. *Diabetes* 51: 1022-1027, 2002.
47. **Sjostrand M, Gudbjornsdottir S, Holmang A, Strindberg L, Ekberg K, and Lonnroth P**. Measurements of interstitial muscle glycerol in normal and insulin-resistant subjects. *J Clin Endocrinol Metab* 87: 2206-2211, 2002.
48. **Song MY, Ruts E, Kim J, Janumala I, Heymsfield S, and Gallagher D**. Sarcopenia and increased adipose tissue infiltration of muscle in elderly African American women. *Am J Clin Nutr* 79: 874-880, 2004.
49. **Terry JG, Shay CM, Schreiner PJ, Jacobs DR, Jr., Sanchez OA, Reis JP, Goff DC, Jr., Gidding SS, Steffen LM, and Carr JJ**. Intermuscular Adipose Tissue and Subclinical Coronary Artery Calcification in Midlife: The CARDIA Study (Coronary Artery Risk Development in Young Adults). *Arterioscler Thromb Vasc Biol* 37: 2370-2378, 2017.
50. **Williams AS, Kang L, and Wasserman DH**. The extracellular matrix and insulin resistance. *Trends in endocrinology and metabolism: TEM* 26: 357-366, 2015.
51. **Yim JE, Heshka S, Albu J, Heymsfield S, Kuznia P, Harris T, and Gallagher D**. Intermuscular adipose tissue rivals visceral adipose tissue in independent associations with cardiovascular risk. *Int J Obes (Lond)* 31: 1400-1405, 2007.

Figure Legends

Figure 1. IMAT conditioned media decreases insulin sensitivity. Conditioned media was generated from SAT, VAT, and IMAT, and administered along with DMEM only control to primary myotubes from obese donors for 3.5 hours at 5% of total media volume. Insulin sensitivity was measured (A), along with changes in the content of 1,2-DAG (B), ceramides (C), dihydroceramides (D), sphingomyelin (E), glucosylceramides (F), and lactosylceramides (G). The FFA content of conditioned media was measured to calculate basal lipolytic rates (H) as well as the composition of individual FFA species (I) from SAT, VAT, and IMAT in culture. Values are means ± SEM. ¥ = significantly different than SAT, # = significantly different than control, $p<0.05$.

Figure 2: IMAT has a unique transcriptome compared to muscle and subcutaneous adipose tissue. MDS plot of logCPM for IMAT, skeletal muscle, and subcutaneous adipose tissue (SAT) samples from RNAseq analyses over dimensions 1 and 2 based on the 1500 most divergent genes. Red = IMAT; blue = muscle; purple = SAT.

Figure 3: Schematic workflow of correlating gene expression with glucose Rd. From the initial 28472 genes we only used genes with at least 25 counts in 70% of the IMAT samples. This left 13476 genes, from which 2222 genes were significantly correlated with GIR ($p < 0.05$). Of these genes, 988 genes correlated negatively and 1234 genes correlated positively with GIR. Additionally, we found 54 KEGG pahtways which showed a correlation with GIR. For more details see text and Methods.

Figure 4: Pathway analysis of human IMAT revealed a down-regulation of key pathways associated with insulin resistance. Green indicates a positive correlation while red indicates a negative correlation between the patient's gene expression and insulin sensitivity. Key genes like the insulin receptor (INSR), the serine-threonine protein kinase (AKT), and the glucose transporter GLUT4 (SLC2A4) were positively associated with insulin sensitivity, and therefore were down-regulated in patients with low insulin sensitivity (A). The MAPK (B) and JAK/STAT (C), signaling pathways were inversely related to insulin sensitivity. Oxidative phosphorylation (D) was associated with insulin sensitivity, and therefore is consistent with mitochondrial dysfunction in insulin resistant individuals.

Figure 5. IMAT macrophage, cytokine, and extracellular matrix gene expression correlates to insulin sensitivity. IMAT mRNA expression of macrophage markers (A), inflammatory cytokines (B), and extracellular matrix proteins (C). Values are means ± SEM. *CD68*, cluster of differentiation 68; *CSF1*, colony stimulating factor 1; *MCP1*, monocyte chemotactic protein 1; *ADAM8*, ADAM metallopeptidase domain 8; *ITGAM*, integrin subunit alpha M; *MSR1*, macrophage scavenger receptor 1; *CSF1R*, colony stimulating Factor 1 Receptor; *MARCO*, Macrophage Receptor With Collagenous Structure; *CD14*, CD14 molecule; CD163, Cluster of Differentiation 163; *ITGAX*, integrin subunit alpha X; *CLEC7A*, C-type lectin domain family 7 member A; *IFNGR1*, interferon

gamma receptor 1; *SIGLEC1*, sialic acid binding Ig like lectin 1; *PAI-1*, plasminogen activator inhibitor type 1; *IL18*, interleukin 18; *TNFAIP3*, TNF alpha induced protein 3; *CXCL12*, stromal cell-derived factor 1; *CCL5*, C-C motif chemokine ligand 5. COL1A1, collagen type I apha 1; COL4A1, collagen type IV alpha 1; *COL5A1*, collagen type V alpha 1; *COL6A1*, collagen type VI alpha 1; *COL21A1*, collagen type XXI alpha 1; *COL24A1* = collagen type XXIV alpha 1; *FN1*, fibronectin 1; *MMP2, 9*, matrix metalloproteinase 2 and 9; *TIMP1-3*, tissue inhibitor of metalloproteinases 1-3; discoidin domain receptor family, member 1, *DDR1*; connective tissue growth factor, *CTGF*; integrin alpha chain 5, ITGAV; integrin alpha L, ITGAL; fibulin 2, FBLN2; fibroblast specific protein, FSP1. § = significantly correlated to insulin sensitivity.

Figure 6. IMAT may influence interstitial FFA concentration promote muscle lipid accumulation. IMAT mRNA expression of genes involved in lipolytic regulation and their relationship to insulin sensitivity (A), and a positive relationship between the KEGG peroxisome pathway and insulin sensitivity (B). *PLIN1* encodes perilipin 1, *PLIN2*, perilipin 2; *PLIN3*, perilipin 3; *PLIN4*, perilipin 4, *PLIN5*, perilipin 5, *ATGL*, adipose triglyceride lipase, *CGI-58*, comparative gene identification-58, *HSL*, hormone sensitive lipase, *MAGL*, monacylglycerol lipase, *FABP4*, fatty acid binding protein 4, *GOS2*, G0/G1 switch 2. § = significantly correlated to insulin sensitivity. Green indicates a positive correlation between the gene expression and insulin sensitivity. Key genes like the sterol carrier protein 2 (SCP2), enoyl-CoA hydratase 1 (ECH1), and ATP binding cassette subfamily D member 1 (ABCD1) were down-regulated in insulin resistant patients.

Figure 7. Conceptual model for IMAT-induced insulin resistance. Potential mechanisms by which IMAT decreases insulin sensitivity in neighboring skeletal muscle.

A

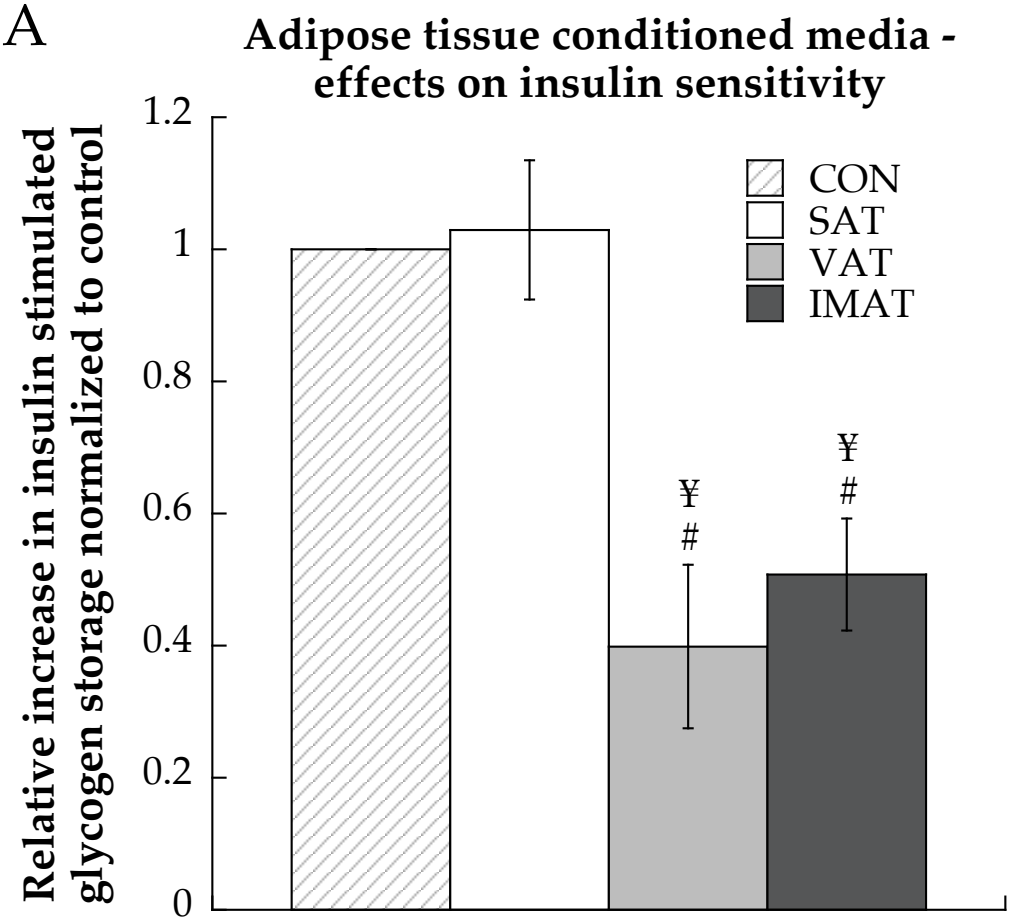

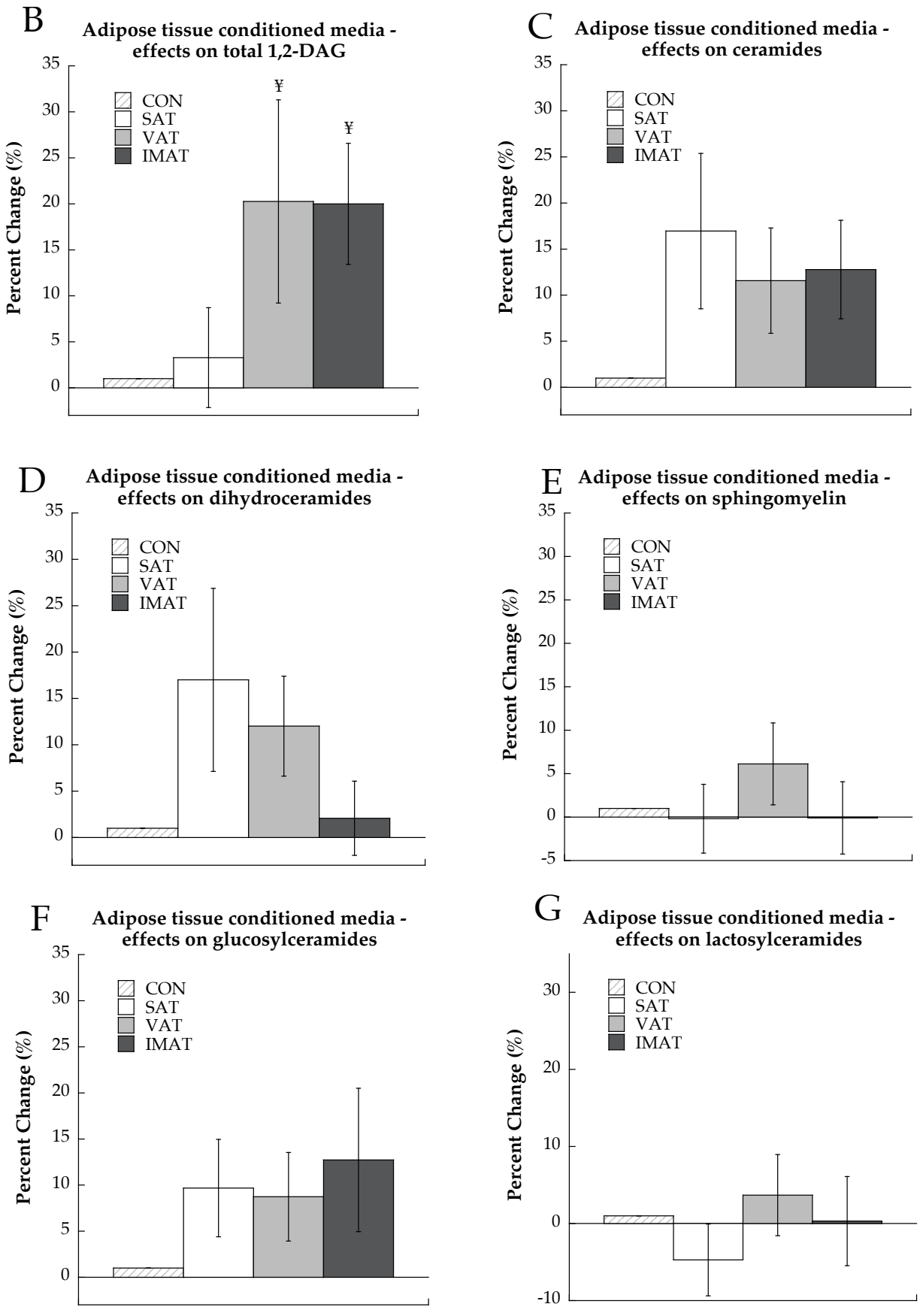

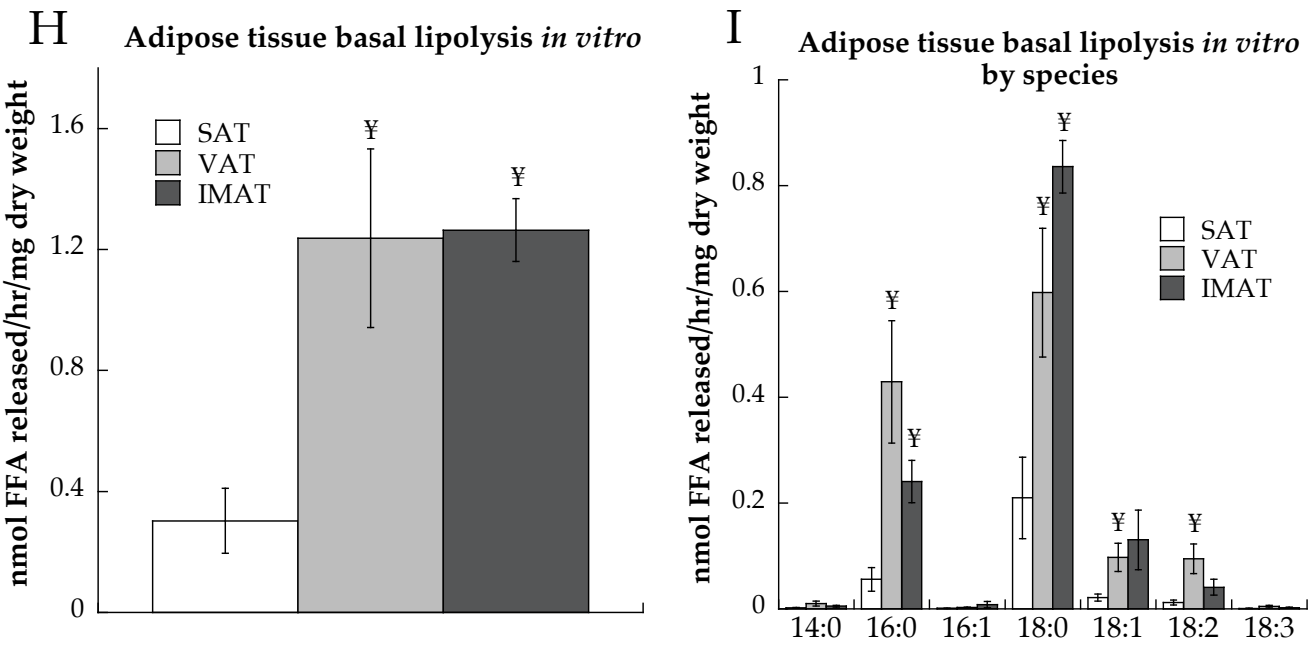

Figure 1. IMAT conditioned media decreases insulin sensitivity. Conditioned media was generated from SAT, VAT, and IMAT, and administered along with DMEM only control to primary myotubes from obese donors for 3.5 hours at 5% of total media volume. Insulin sensitivity was measured (A), along with changes in the content of 1,2-DAG (B), ceramides (C), dihydroceramides (D), sphingomyelin (E), glucosylceramides (F), and lactosylceramides (G). The FFA content of conditioned media was measured to calculate basal lipolytic rates (H) as well as the composition of individual FFA species (I) from SAT, VAT, and IMAT in culture. Values are means ± SEM. ¥ = significantly different than SAT, # = significantly different than control, $p<0.05$.

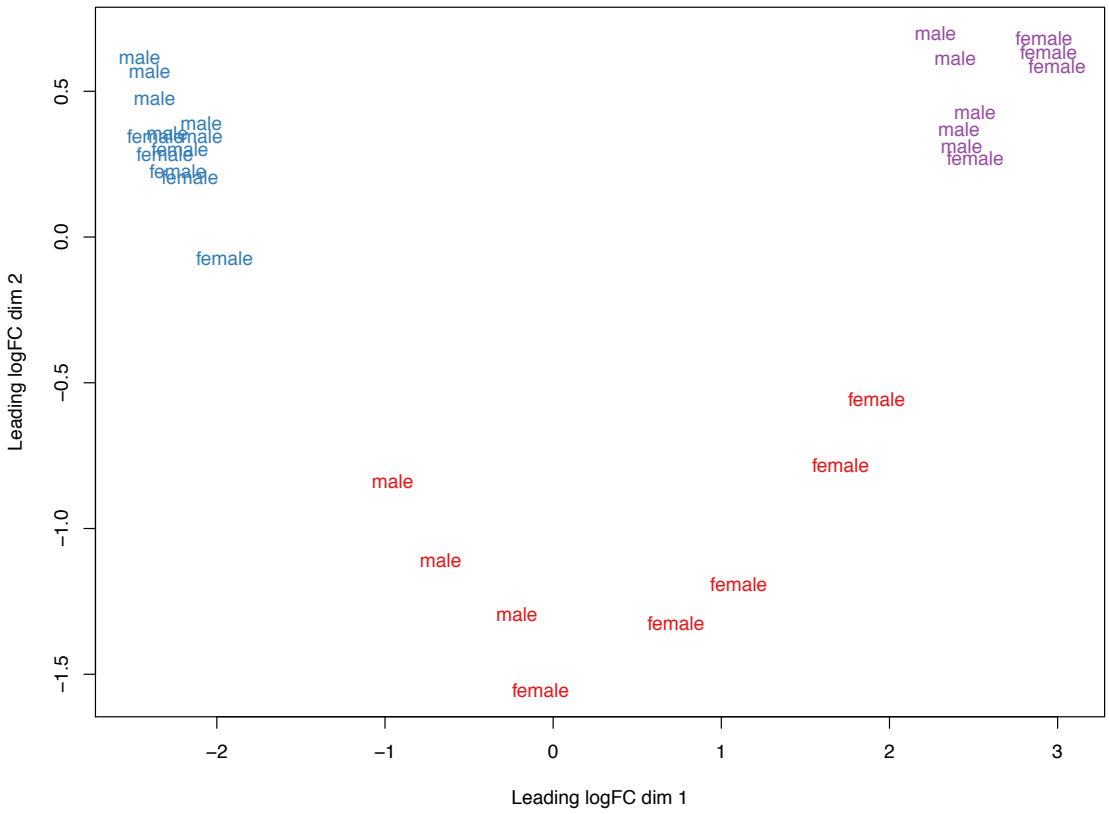

Figure 2: IMAT has a unique transcriptome compared to muscle and subcutaneous adipose tissue. MDS plot of logCPM for IMAT, skeletal muscle, and subcutaneous adipose tissue (SAT) samples from RNAseq analyses over dimensions 1 and 2 based on the 1500 most divergent genes. Red = IMAT; blue = muscle; purple = SAT.

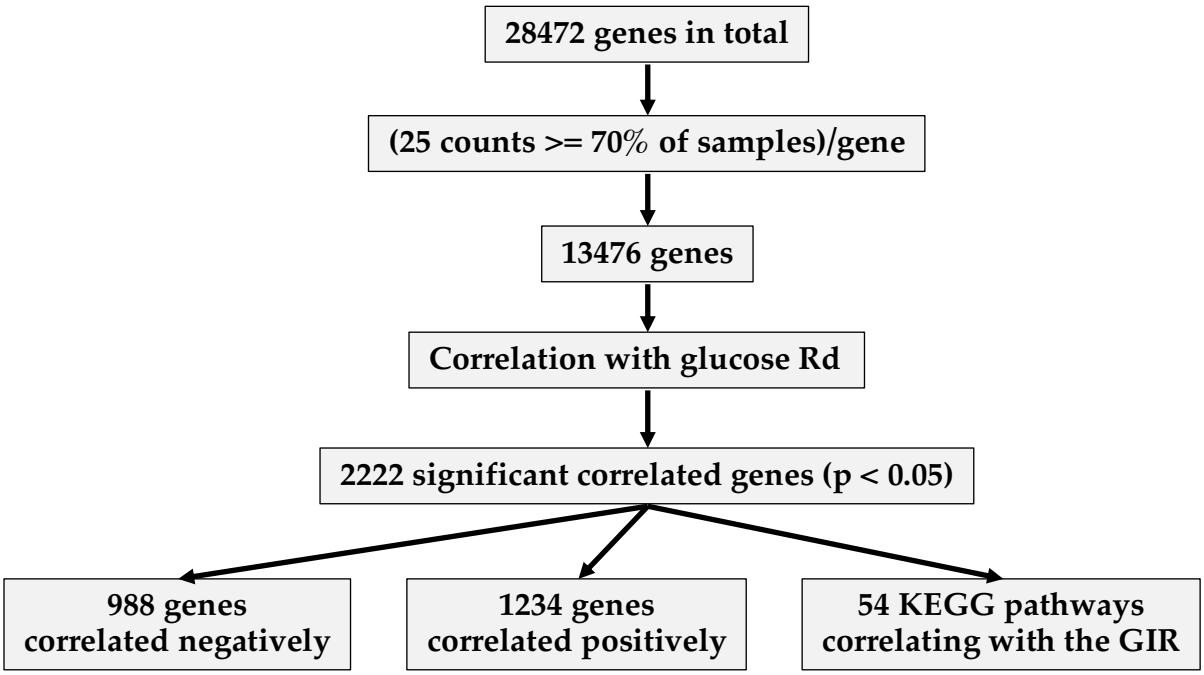

Figure 3: Schematic workflow of correlating gene expression with glucose Rd. From the initial 28472 genes we only used genes with at least 25 counts in 70% of the IMAT samples. This left 13476 genes, from which 2222 genes were significantly correlated with GIR ($p < 0.05$). Of these genes, 988 genes correlated negatively and 1234 genes correlated positively with GIR. Additionally, we found 54 KEGG pahtways which showed a correlation with GIR. For more details see text and Methods.

A

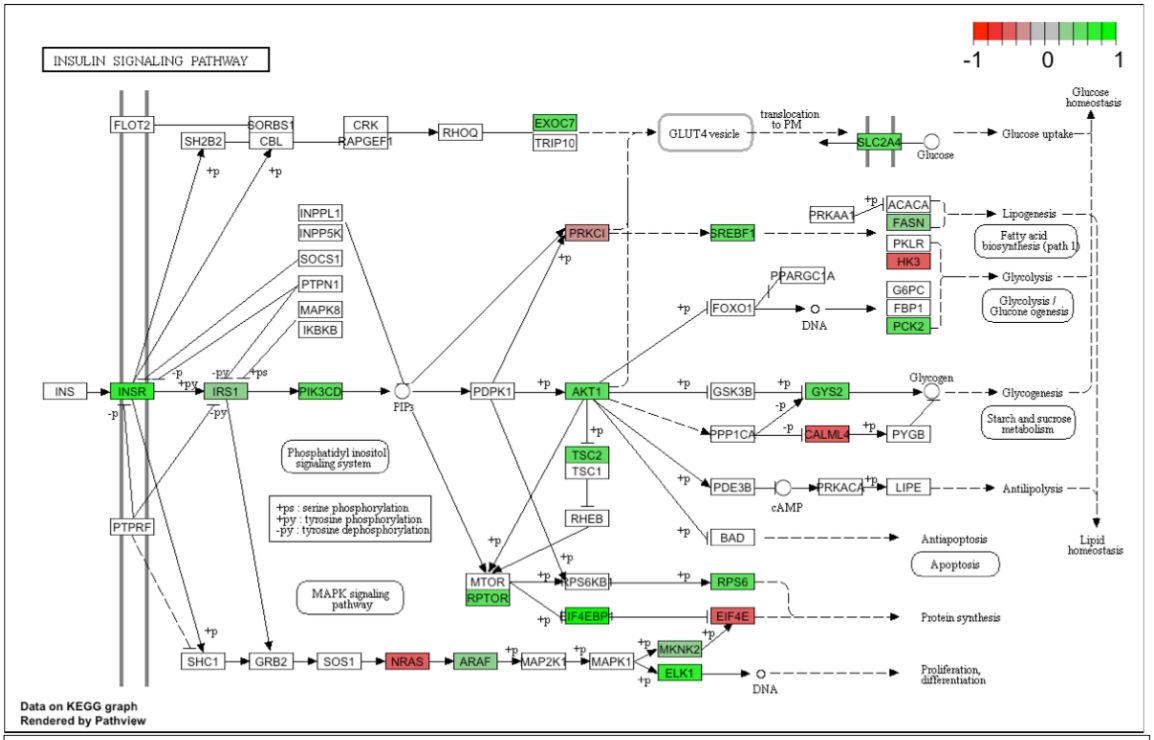

B

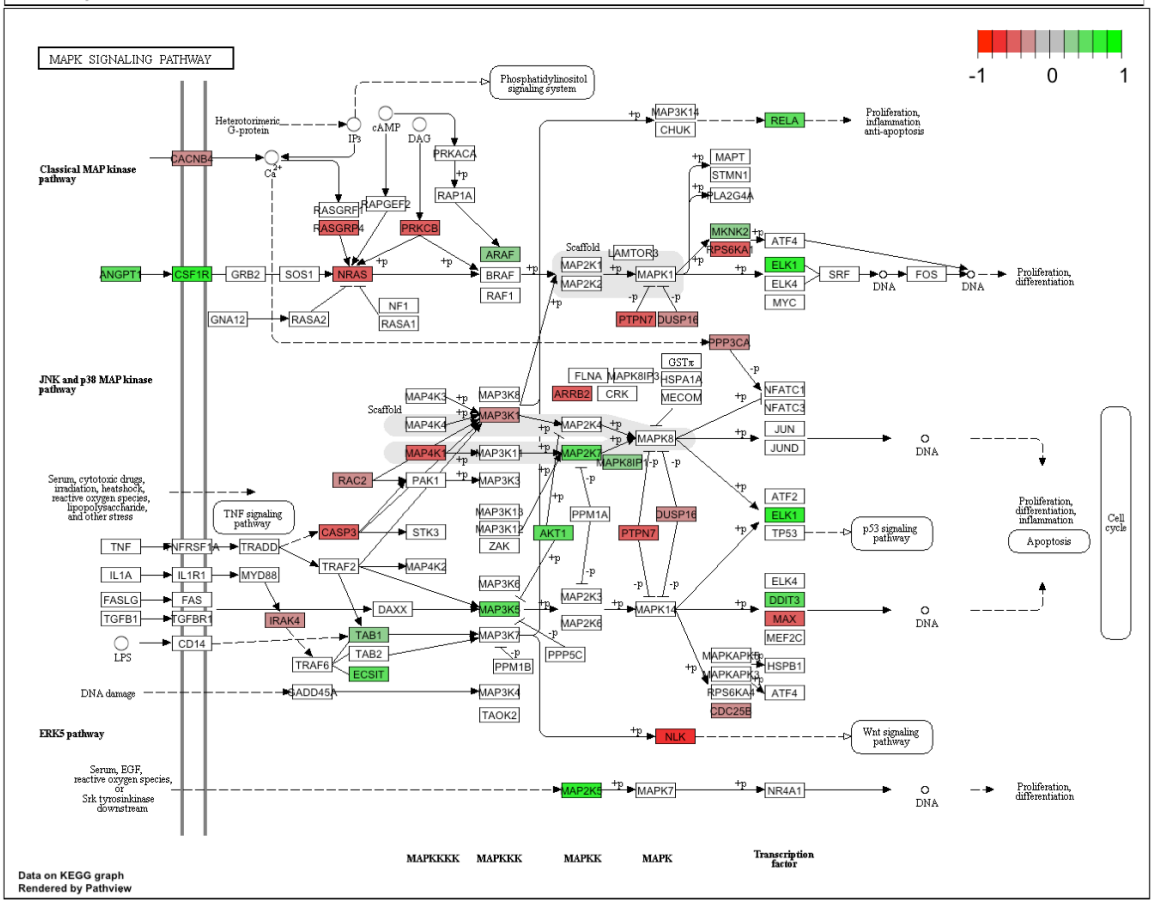

C

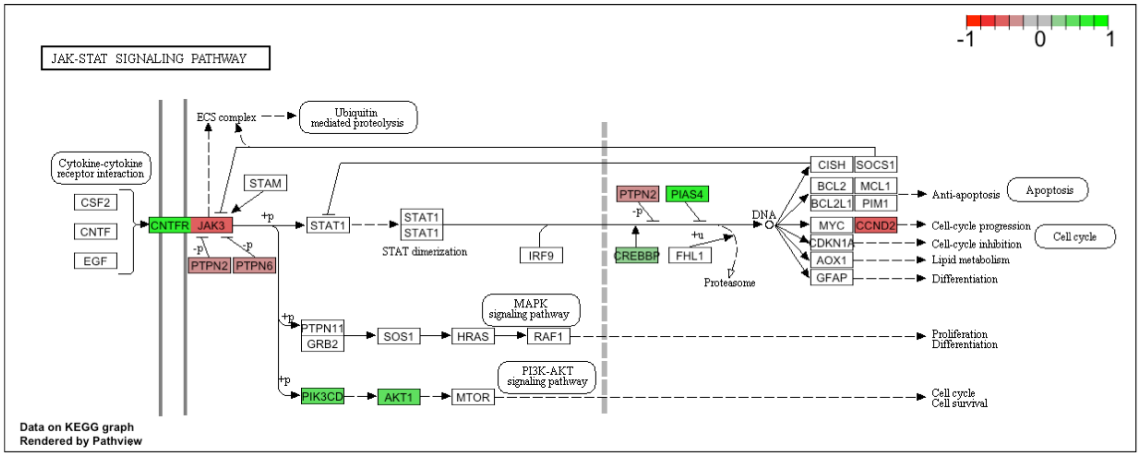

D

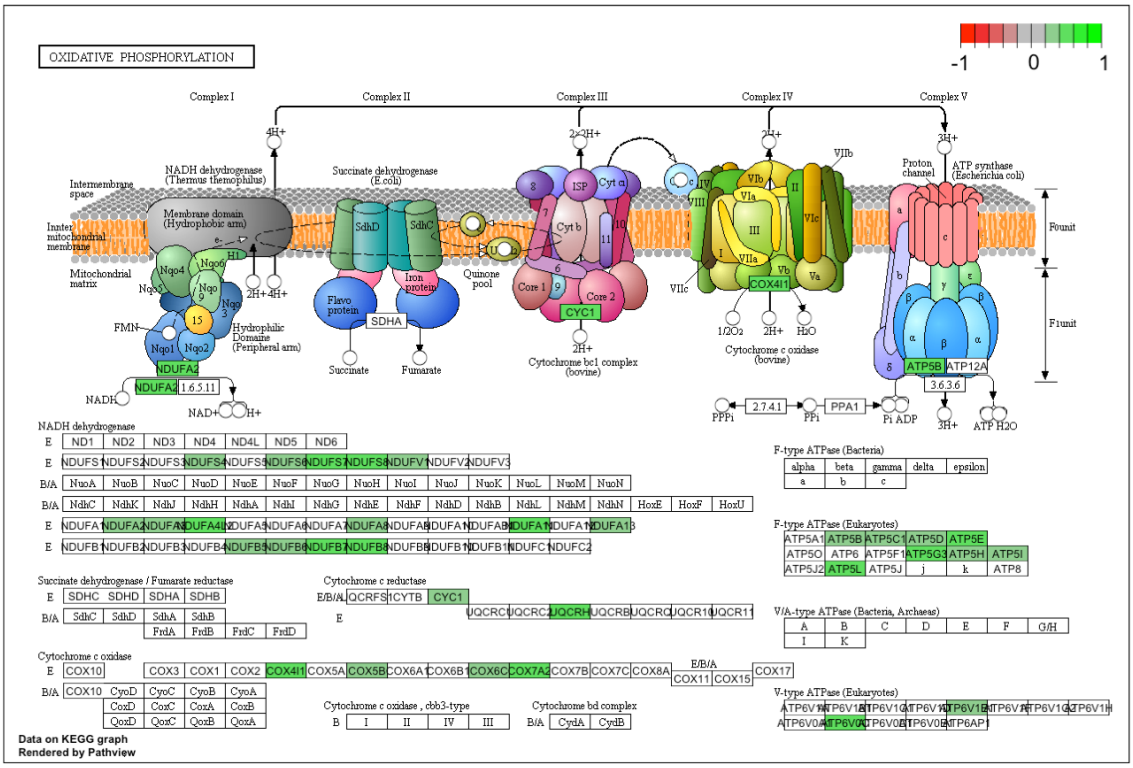

Figure 4: Pathway analysis of human IMAT revealed a down-regulation of key pathways associated with insulin resistance. Green indicates a positive correlation while red indicates a negative correlation between the patient's gene expression and insulin sensitivity. Key genes like the insulin receptor (INSR), the serine-threonine protein kinase (AKT), and the glucose transporter GLUT4 (SLC2A4) were positively associated with insulin sensitivity, and therefore were down-regulated in patients with low insulin sensitivity (A). The MAPK (B) and JAK/STAT (C), signaling pathways were inversely related to insulin sensitivity. Oxidative phosphorylation (D) was associated with insulin sensitivity, and therefore is consistent with mitochondrial dysfunction in insulin resistant individuals.

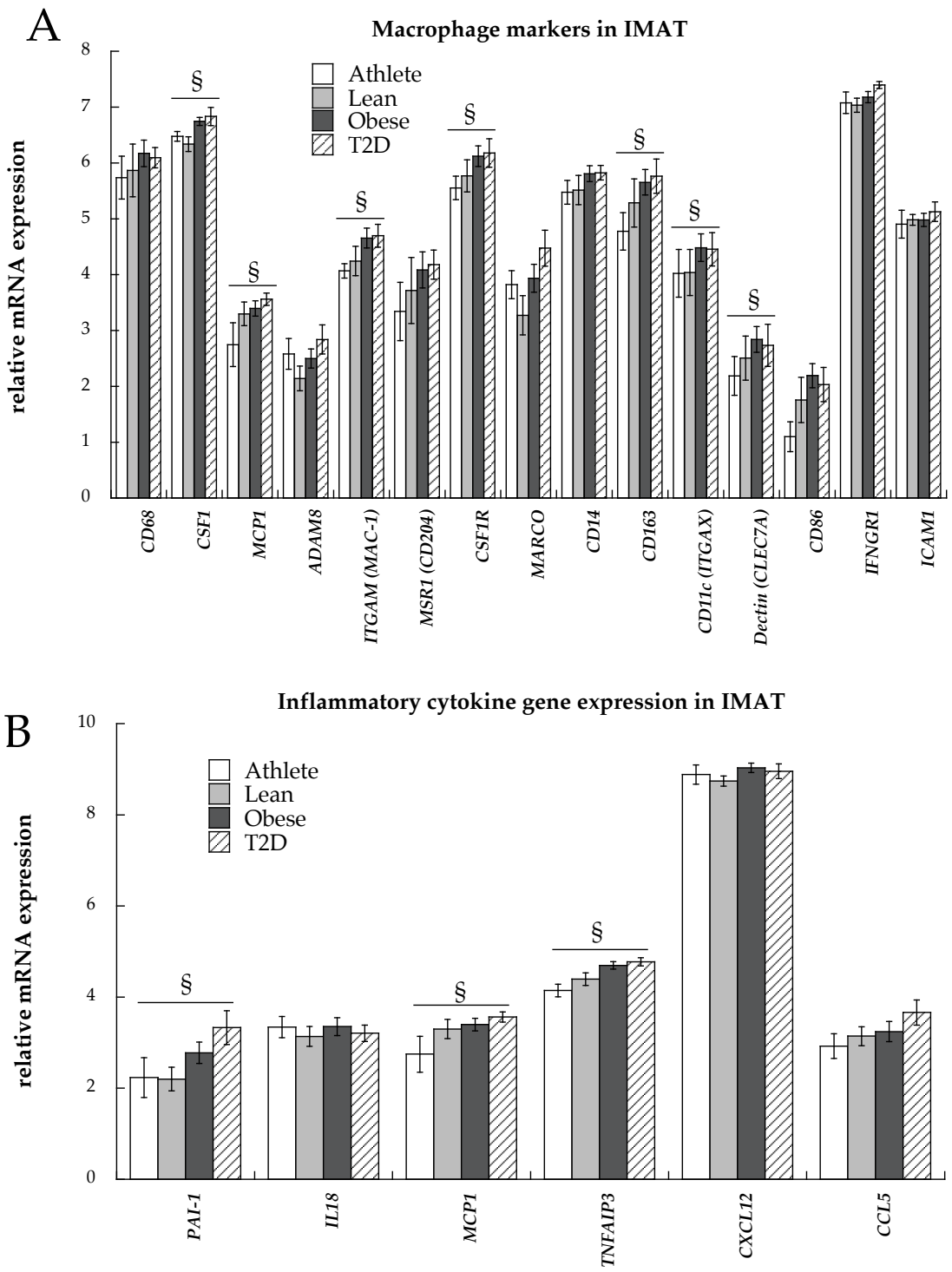

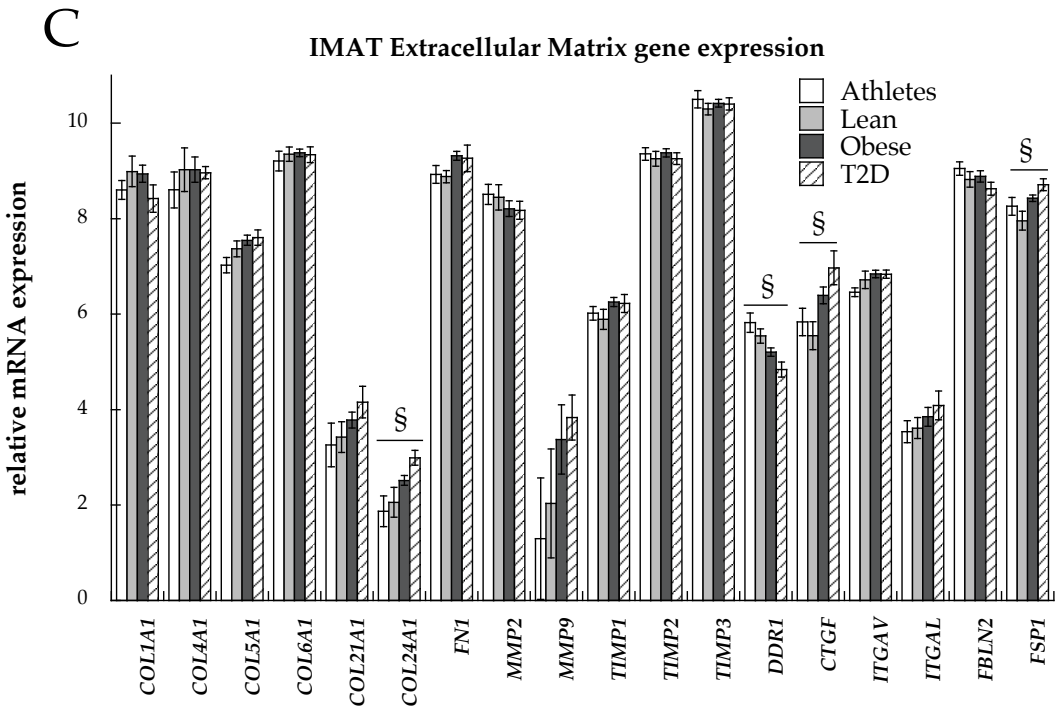

Figure 5. IMAT macrophage, cytokine, and extracellular matrix gene expression correlates to insulin sensitivity. IMAT mRNA expression of macrophage markers (A), inflammatory cytokines (B), and extracellular matrix proteins (C). Values are means ± SEM. *CD68*, cluster of differentiation 68; *CSF1*, colony stimulating factor 1; *MCP1*, monocyte chemotactic protein 1; *ADAM8*, ADAM metallopeptidase domain 8; *ITGAM*, integrin subunit alpha M; *MSR1*, macrophage scavenger receptor 1; *CSF1R*, colony stimulating Factor 1 Receptor; *MARCO*, Macrophage Receptor With Collagenous Structure; *CD14*, CD14 molecule; CD163, Cluster of Differentiation 163; *ITGAX*, integrin subunit alpha X; *CLEC7A*, C-type lectin domain family 7 member A; *IFNGR1*, interferon gamma receptor 1; *SIGLEC1*, sialic acid binding Ig like lectin 1; *PAI-1*, plasminogen activator inhibitor type 1; *IL18*, interleukin 18; *TNFAIP3*, TNF alpha induced protein 3; *CXCL12*, stromal cell-derived factor 1; *CCL5*, C-C motif chemokine ligand 5. COL1A1, collagen type I apha 1; COL4A1, collagen type IV alpha 1; *COL5A1*, collagen type V alpha 1; *COL6A1*, collagen type VI alpha 1; *COL21A1*, collagen type XXI alpha 1; *COL24A1*, collagen type XXIV alpha 1; *FN1*, fibronectin 1; *MMP2, 9*, matrix metalloproteinase 2 and 9; *TIMP1-3*, tissue inhibitor of metalloproteinases 1-3; discoidin domain receptor family, member 1, *DDR1*; connective tissue growth factor, *CTGF*; integrin alpha chain 5, ITGAV; integrin alpha L, ITGAL; fibulin 2, FBLN2; fibroblast specific protein, FSP1. § = significantly correlated to insulin sensitivity.

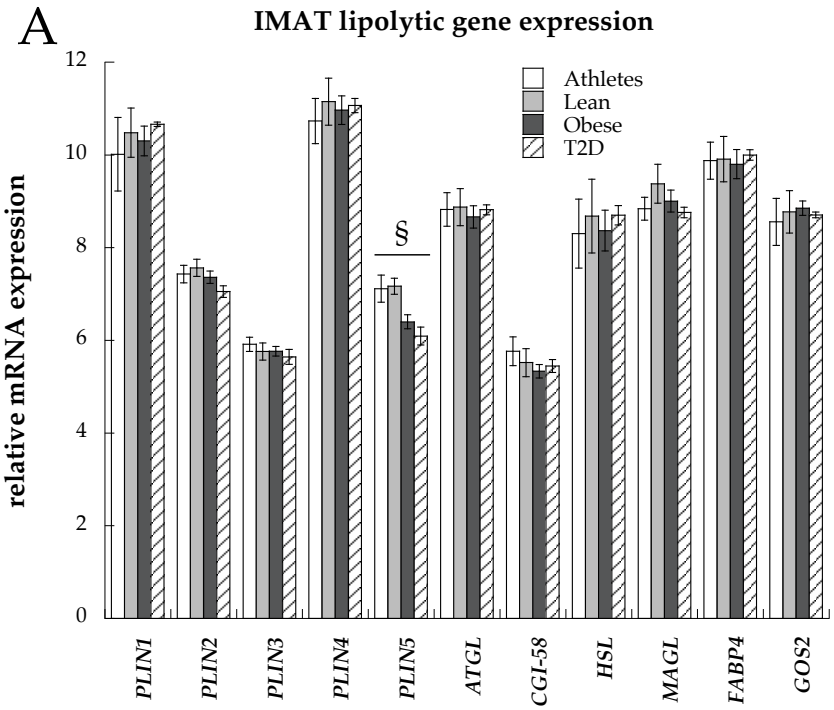

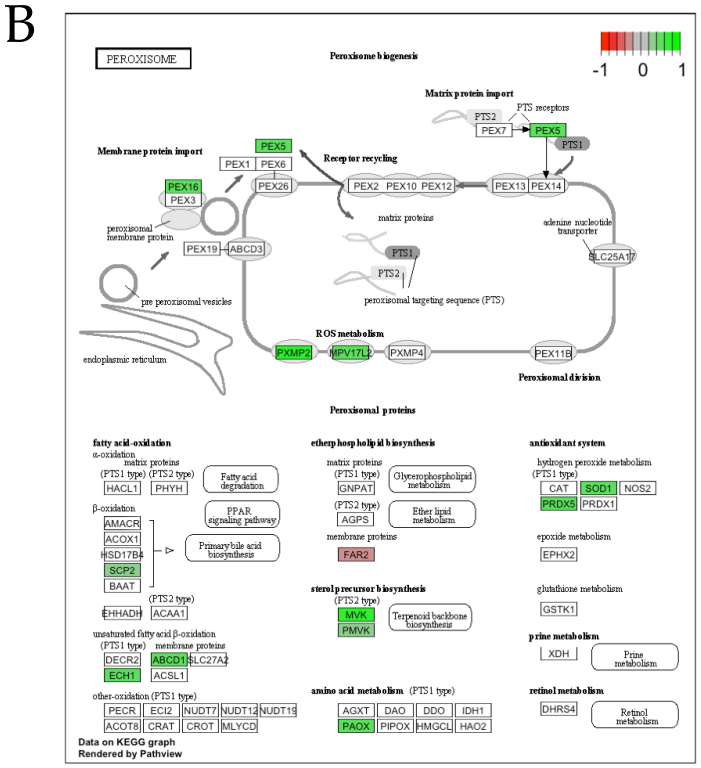

Figure 6. IMAT may influence interstitial FFA concentration promote muscle lipid accumulation. IMAT mRNA expression of genes involved in lipolytic regulation and their relationship to insulin sensitivity (A), and a positive relationship between the KEGG peroxisome pathway and insulin sensitivity (B). *PLIN1* encodes perilipin 1, *PLIN2*, perilipin 2; *PLIN3*, perilipin 3; *PLIN4*, perilipin 4, *PLIN5*, perilipin 5, *ATGL*, adipose triglyceride lipase, *CGI-58*, comparative gene identification-58, *HSL*, hormone sensitive lipase, *MAGL*, monacylglycerol lipase, *FABP4*, fatty acid binding protein 4, *GOS2*, G0/G1 switch 2. § = significantly correlated to insulin sensitivity. Green indicates a positive correlation between the gene expression and insulin sensitivity. Key genes like the sterol carrier protein 2 (SCP2), enoyl-CoA hydratase 1 (ECH1), and ATP binding cassette subfamily D member 1 (ABCD1) were down-regulated in insulin resistant patients.

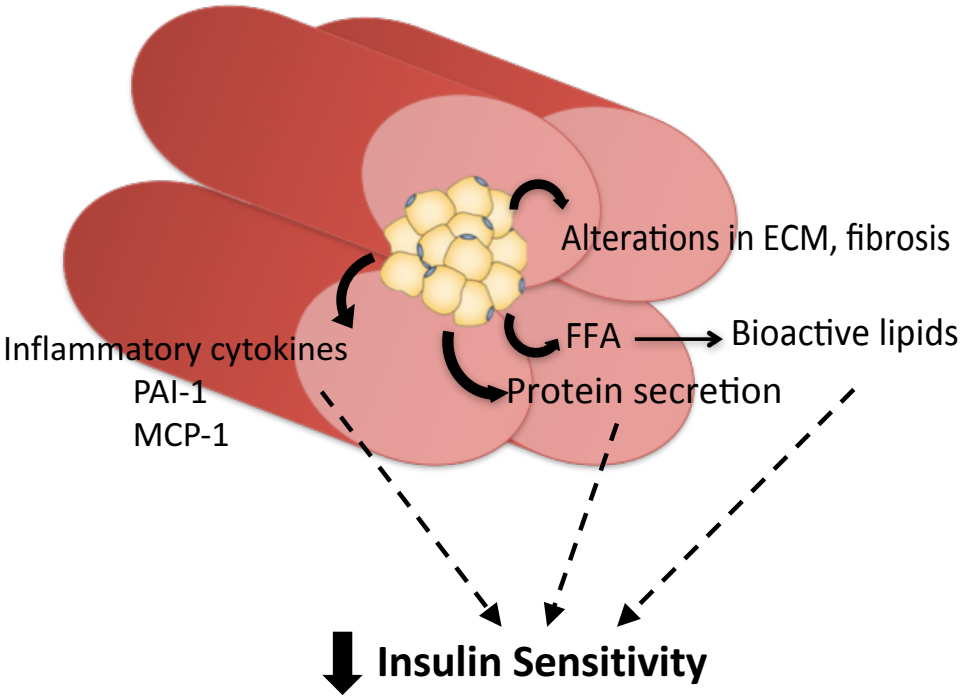

Figure 7. Conceptual model for IMAT-induced insulin resistance. Potential mechanisms by which IMAT decreases insulin sensitivity in neighboring skeletal muscle.